

A FIRST LOOK AT ROTATION IN INACTIVE LATE-TYPE M DWARFS

ANDREW A. WEST^{1,2,3}, GIBOR BASRI²

Draft version November 5, 2018

ABSTRACT

We have examined the relationship between rotation and activity in 14 late-type (M6-M7) M dwarfs, using high resolution spectra taken at the W.M. Keck Observatory and flux-calibrated spectra from the Sloan Digital Sky Survey. Most were selected to be inactive at a spectral type where strong H α emission is quite common. We used the cross-correlation technique to quantify the rotational broadening; six of the stars in our sample have $v \sin i \geq 3.5 \text{ km s}^{-1}$. Our most significant and perplexing result is that three of these stars do not exhibit H α emission, despite rotating at velocities where previous work has observed strong levels of magnetic field and stellar activity. Our results suggest that rotation and activity in late-type M dwarfs may not always be linked, and open several additional possibilities including a rotationally-dependent activity threshold, or a possible dependence on stellar parameters of the Rossby number at which magnetic/activity “saturation” takes place in fully convective stars.

Subject headings: stars: low-mass, brown dwarfs — stars: activity — stars: late-type — stars: rotation

1. INTRODUCTION

Many M dwarfs, which are the most abundant stars in the Milky Way, have strong magnetic dynamos that give rise to chromospheric and coronal heating, producing emission from the X-ray to the radio. Although this magnetic heating (or activity) has been observed for decades, the exact mechanisms that control magnetic activity in M dwarfs are still not well-understood. In the Sun, magnetic fields are generated at the boundary between the convective and the radiative zones (known as the tachocline), where the differential rotation in the convective zone creates a rotational shear (Parker 1993; Ossendrijver 2003; Thompson et al. 2003) that allows magnetic fields to be generated, stored and ultimately rise to the surface. These fields drive the heating of the stellar chromosphere and corona, resulting in both flares and lower level quiescent magnetic activity. A common diagnostic of this heating in optical spectra (of M dwarfs) is the H α emission line.

Rotation in solar-type stars slows with time due to angular momentum loss from magnetized stellar winds; as a result, magnetic activity decreases. Skumanich (1972) found that both activity (as measured by Ca II emission) and projected rotational velocity decrease over time as a power law ($t^{-0.5}$). Subsequent studies confirmed the Skumanich results and demonstrated that there is a strong link between age, rotation and activity in Solar-type stars (Barry 1988; Soderblom et al. 1991; Pizzolato et al. 2003; Mamajek & Hillenbrand 2008).

There is strong evidence that the rotation-activity relation extends from stars more massive than the Sun to smaller dwarfs (Pizzolato et al. 2003; Mohanty & Basri 2003; Kiraga & Stepień 2007). However, at a spectral type of \sim M3 (0.35 M_{\odot} ; Reid & Hawley 2005; Chabrier & Baraffe 1997)⁴, stars become fully convective and the

tachocline presumably disappears. This transition marks an important change in the stellar interior that has been thought to affect the production and storage of internal magnetic fields. Despite this change in the stellar interiors, magnetic activity persists in the late-type M dwarfs; the fraction of active stars peaks around a spectral type of M7 before decreasing into the brown dwarf regime (Hawley et al. 1996; Gizis et al. 2000; West et al. 2004).

A few previous studies of H α emission have uncovered evidence of a possible rotation-activity relation extending past the M3 convective transition and into the brown dwarf regime (Delfosse et al. 1998; Mohanty & Basri 2003; Reiners & Basri 2007). In addition, recent simulations of magnetic dynamo generation in fully convective stars find that rotation may play a role in magnetic field generation (Dobler et al. 2006; Browning 2008). However, the lack of an unbiased sample of high resolution spectra of late-type M dwarfs complicates the situation.

Using over 30000 spectra from the Sloan Digital Sky Survey (SDSS; Adelman-McCarthy et al. 2008), West et al. (2006, 2008) showed that the activity fraction of M dwarfs varies as a function of stellar age (using Galactic height as a proxy for age) and that the H α activity lifetime for M6-M7.5 stars is 7-8 Gyr. Nearby samples of late-type M dwarfs are therefore biased towards young populations with high levels of activity; until recently every known M7 dwarf was observed to be magnetically active (Hawley et al. 1996; Gizis et al. 2000; West et al. 2004).

Due to the intrinsic faintness of late-type M dwarfs, previous rotation studies were limited (and therefore biased) toward, bright, nearby, and therefore active M dwarfs; the 21 M6-M7.5 dwarfs that have previous rotation measurements are all active (Delfosse et al. 1998; Mohanty & Basri 2003; Reiners & Basri 2007). The advent of large spectroscopic surveys of M dwarfs (e.g. SDSS) allows for improved sample selection that can

and migrate across a range of spectral types while at the same stellar mass; mass and spectral type are only coupled in stars that have settled on the main sequence ($> 500 \text{ Myr}$ for most late-type M dwarfs).

¹ Corresponding author: aaw@space.mit.edu

² Astronomy Department, University of California, 601 Campbell Hall, Berkeley, CA 94720-3411

³ MIT Kavli Institute for Astrophysics and Space Research, 77 Massachusetts Ave, 37-582c, Cambridge, MA 02139-4307

⁴ Although mass and spectral type are closely linked in evolved low-mass dwarfs, young, low-mass objects cool rapidly with age

minimize observational bias in the study of late-type M dwarfs.

In this paper we present results from our study of the *vsini* rotation velocities for a small sample of M6-M7 dwarfs, most of which were selected to be inactive or weakly active from the SDSS low-mass star spectroscopic sample. We describe the sample and observations in §2, our analysis in §3, and the observational results in §4. We then discuss our results in §5.

2. DATA

Our sample was selected from the West et al. (2008) Sloan Digital Sky Survey (SDSS) M dwarf catalog, a spectroscopic sample of almost 40000 M and L-type dwarfs. We selected the brightest M6 and M7 stars which were either inactive ($H\alpha$ equivalent width < 0.3) or weakly active ($H\alpha$ equivalent width < 1.0). 12 stars were selected using these criteria. Two additional active ($H\alpha$ equivalent width > 1.0) M7 dwarfs were added to the sample for comparison to previous studies. While our sample is not a complete unbiased sample, representative of the underlying M dwarf population, it does consist of late-type M dwarfs with activity properties selectively different than previously observed.

The 14 stars were observed during four observing runs (13 October 2006, 14 October 2006, 25 April 2007, and 24 January 2008) using the HIRES spectrograph at Keck I. Our setup covered the wavelength region from 5600 to 10000 Å with a resolution of $R \sim 30000$. The data were reduced with standard IDL routines that included flat-fielding, sky subtraction and cosmic ray removal. In addition to our 14 program stars, we observed the nearby M6 dwarf Gl406, a star with no measurable rotation (Delfosse et al. 1998; Mohanty & Basri 2003) that we used as a zero rotation velocity template.

3. ANALYSIS

3.1. Rotation from Cross Correlation

To measure the *vsini* rotation velocities for our sample, we used a cross-correlation technique similar to that of previous studies (e.g. Delfosse et al. 1998; Mohanty & Basri 2003): we cross-correlated each program spectrum with the spectrum of a slowly rotating comparison star. The width of the resulting cross correlation function is a direct probe of the rotational broadening.

We used Gl 406 (M6) as our template because it has a similar spectral type to our sample as well as a small (non detectable) rotation velocity (Delfosse et al. 1998; Mohanty & Basri 2003). Four wavelength regions with strong molecular bands were used to compute independent cross-correlation functions: 6700-6760 Å, 7080-7140 Å, 8430-8500 Å (adapted from Browning et al. 2008), and 9946-9956 Å (Reiners 2007). Figure 1 shows an example of all four regions from one of the stars in our sample (SDSS094738.45+371016.5). The S/N ranges from 10-60 in all of the spectral regions for all of the stars. The three bluer spectral windows yielded good cross-correlation functions that were consistent with each other for all 14 program stars. In contrast, only a few good solutions were produced using the 9946-9956 Å window. The problem with this spectral window may be due to the mix of broad and narrow FeH features in the 9946-9956 Å region; this region is more amenable to a

spectral fitting approach to measure rotational broadening (e.g. Reiners 2007). Gl 406 is an active M6 dwarf with a strong magnetic field (Reiners & Basri 2007), and the FeH region is also sensitive to magnetic effects. To alleviate this problem, we followed the same cross-correlation procedure but instead used one of our non rotating (based on the other 3 spectral regions) program stars, SDSS125855.13+052034.7 to cross correlate with the sample spectra. Using this template, we were able to get better cross-correlation functions for the 9946-9956 Å region.

To measure the rotational broadening of each spectrum, we compared the resulting cross-correlation function to that of a rotationally broadened template. The Gl 406 and SDSS125855.13+052034.7 templates were rotationally broadened to larger rotation velocities using the technique of Gray (1992) and cross-correlated with the original (unbroadened) template in 0.5 km s^{-1} intervals. The resulting spun-up cross-correlation functions were compared with the cross-correlation functions of the sample spectra and a *vsini* was determined based on the best fit spun-up template. Figure 2 shows the cross-correlation function of SDSS094738.45+371016.5 with Gl406 in the 7080-7140 Å region (solid) compared with the cross-correlation function of Gl406 with the best-fit rotationally broadened Gl406 spectrum (dotted; 6 km s^{-1}), and the auto-correlation function of Gl406 (dashed; 0 km s^{-1} broadening). The cross-correlation reveals that SDSS094738.45+371016.5 appears to be rotating with a velocity $\geq 6 \text{ km s}^{-1}$.

No detectable difference was seen between the non-rotating template and the spun-up templates with $V_{\text{rot}} \leq 3.5 \text{ km s}^{-1}$ for the S/N of our typical spectra. We therefore used 4 km s^{-1} as our threshold for detectable rotation in this paper. The *vsini* values from each spectral window were averaged and the resulting value for each star is reported in Table 1. For stars with multiple spectra, the *vsini* values in Table 1 represent the average of all spectral windows for all observations. The *vsini* variation amongst spectral windows and multiple observations was always within the 0.5 km s^{-1} bin size. We therefore used 0.5 km s^{-1} as the uncertainty in the *vsini* measurements.

3.2. Spectral Analysis

3.2.1. Activity

All of the spectra were spectral typed by eye using the Hammer spectral analysis package (Covey et al. 2007) on the SDSS spectra. We measured the equivalent widths (EW) of the $H\alpha$ emission lines in both the SDSS and Keck spectra. The Keck spectra are more sensitive to low levels of emission; they can be distinguished better against the pervasive molecular features. Our EWs are really psuedo-EWs, since there is no real continuum in the spectra. This has different effects at low and high resolution, which is one reason that EWs tend to be smaller when measured from high resolution spectra. Almost all of our targets chosen to be inactive at low resolution proved inactive even at high resolution, and the EWs when detected were similar. In one case (SDSS083231.52+474807.7), the high resolution spectrum seems to have caught a small flare. Figure 3 shows the SDSS and Keck spectra of the inactive M7

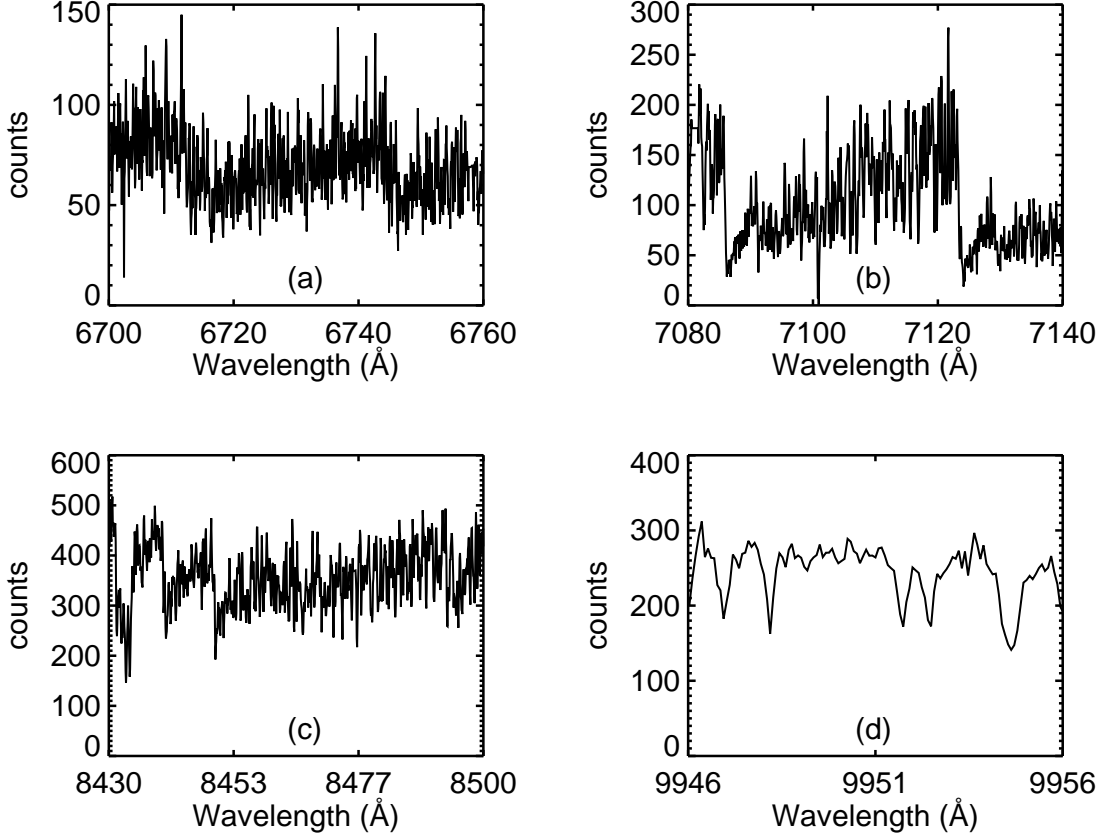


FIG. 1.— Keck spectra of SDSS094738.45+371016.5 in the four spectral regions used for cross-correlation: (a) 6700-6760 Å, (b) 7080-7140 Å, (c) 8430-8500 Å, and (d) 9946-9956 Å.

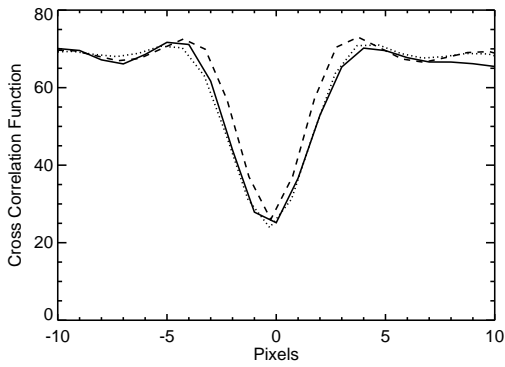


FIG. 2.— Cross correlation function of SDSS094738.45+371016.5 with G1406 in the 7080-7140 Å region (solid) compared with the cross-correlation function of G1406 with the best-fit rotationally broadened G1406 spectrum (dotted; 6 km s^{-1}), and the auto-correlation function of G1406 (dashed; 0 km s^{-1} broadening). The cross-correlation reveals that SDSS094738.45+371016.5 appears to be rotating with a velocity $\geq 6 \text{ km s}^{-1}$ despite not having any signs of activity in either the SDSS or Keck spectra.

dwarf SDSS094738.45+371016.5 (a and b respectively) and the active M7 dwarf SDSS162718.20+353835.7 (c and d). Dashed lines in the SDSS spectra (a and c) indicate the expected position of the $\text{H}\alpha$ emission line. The inset panels in the SDSS spectra are zoomed in on

the $\text{H}\alpha$ region (6500-6600 Å). Despite their high quality, it is clear that no $\text{H}\alpha$ emission is detected in either of the inactive spectra.

We also measured the $\text{H}\beta$, $\text{H}\gamma$, $\text{H}\delta$, and CaII K emission lines from the SDSS spectra. The EW values are presented in Table 1. For the stars in which no lines were detected, we computed EW upper limits based on the required EW needed to detect an emission line at the 3σ confidence level. These are also reported in Table 1. Using the relations from Walkowicz et al. (2004, $\text{H}\alpha$) and West & Hawley (2008, other lines), we converted the EWs and upper limits for all of the lines to fractions of the bolometric luminosity (e.g. $L_{\text{H}\alpha}/L_{\text{bol}}$, etc.). The $L_{\text{line}}/L_{\text{bol}}$ values are presented in Table 2.

We estimated the Rossby number ($R_0 = \text{Period}/\tau_c$) for the 6 stars with measured rotation velocities, following the prescription of Reiners et al. (2008, $\tau_c = 70$ days), and assuming stellar radii of $0.12 R_\odot$ and $0.1 R_\odot$ for M6 and M7 dwarfs respectively (Reid & Hawley 2005). Our estimated R_0 values are included in Table 1. All of the estimated Rossby numbers are in the regime of activity “saturation” ($R_0 < 0.1$) described in Reiners et al. (2008).

3.2.2. Metallicity

We measured the TiO5 , CaH2 , and CaH3 molecular band indices (Reid et al. 1995) from the SDSS spectra, features that probe the relative metallicities of M

TABLE 1
MEASURED ATTRIBUTES

Name	Sp. Type	$v \sin i$ (km s^{-1})	$\text{H}\alpha^a$	$\text{H}\alpha^b$	Equivalent Width (\AA)			CaII K^a	TiO5^c	CaH2^c	CaH3^c	Rossby Num.
SDSS011012.22+085627.5	M7	<3.5	<0.2	<0.2	<0.6	<1.7	<4.3	<0.9	0.17	0.27	0.56	...
SDSS021749.99+084409.4	M6	4.0 ± 0.5	<0.1	<0.1	<0.4	<2.2	<1.7	<0.8	0.28	0.35	0.67	0.03
SDSS023908.41+072429.3	M7	<3.5	<0.1	0.3	<0.8	<7.0	0.23	0.32	0.61	...
SDSS072543.94+382511.4	M7	<3.5	<0.1	<0.1	<0.2	<0.5	<0.5	<1.1	0.27	0.35	0.67	...
SDSS083231.52+474807.7	M6	4.0 ± 0.5	<0.1	3.9^d	<0.2	<0.5	<0.5	1.1	0.28	0.34	0.64	0.03
SDSS094720.07+002009.5	M7	6.5 ± 0.5	3.4	4.0	4.2	17.2	2.6	12.2	0.22	0.28	0.57	0.01
SDSS094738.45+371016.5	M7	6.0 ± 0.5	<0.2	<0.1	<0.2	<0.9	<1.8	<1.0	0.19	0.27	0.59	0.01
SDSS110153.86+341017.1	M7	<3.5	<0.2	<0.1	<0.2	<1.1	<1.1	<0.8	0.22	0.29	0.60	...
SDSS112036.08+072012.7	M7	<3.5	<0.1	<0.1	<0.2	<0.3	<0.4	<0.5	0.26	0.32	0.66	...
SDSS125855.13+052034.7	M7	<3.5	0.9	<0.1	1.8	7.2	4.5	5.8	0.25	0.31	0.62	...
SDSS151727.72+335702.4	M7	4.5 ± 0.5	<0.2	<0.1	<0.2	<0.6	<0.8	<0.3	0.26	0.35	0.70	0.02
SDSS162718.20+353835.7	M7	8.0 ± 0.5	5.9	5.4	19.7	37.1	32.4	26.5	0.24	0.20	0.61	0.01
SDSS220334.10+130839.8	M7	<3.5	<0.1	<0.1	<0.6	<2.8	<2.3	<2.3	0.22	0.32	0.66	...
SDSS225228.50+101910.9	M7	<3.5	<0.2	<0.2	<0.7	<9.8	0.19	0.26	0.59	...

^aEquivalent width or 3σ upper limit measured from the SDSS spectrum

^bEquivalent width or 3σ upper limit measured from the Keck spectrum

^cBandhead measured from the SDSS spectrum

^dKeck spectrum observed during a small flare

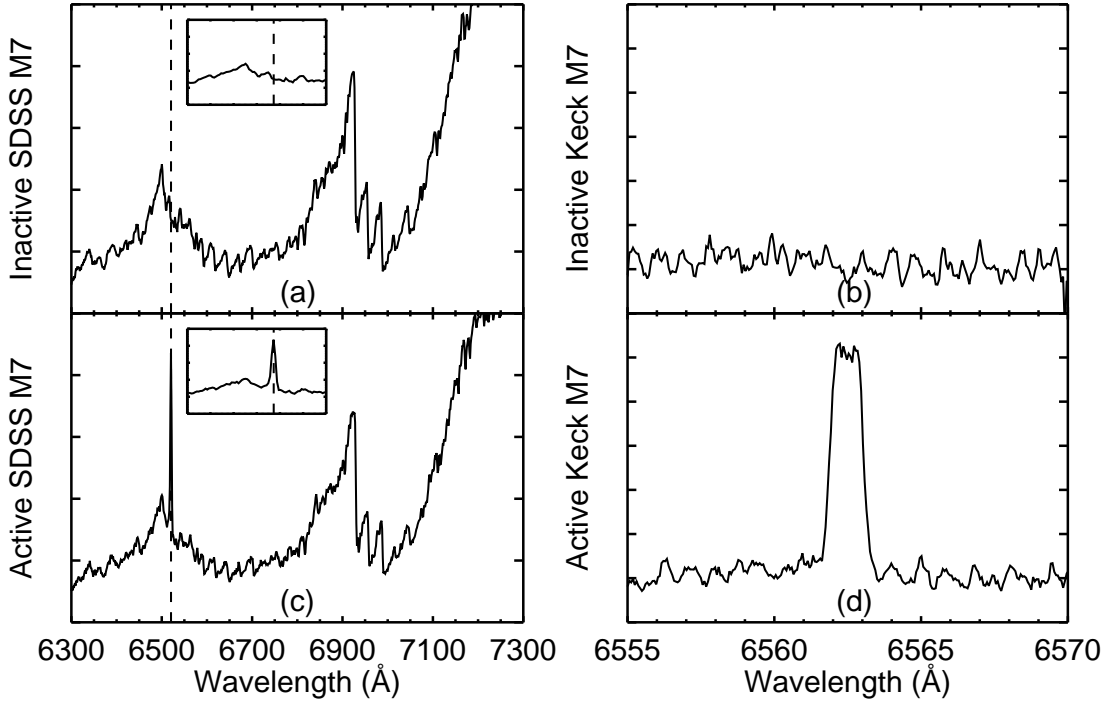


FIG. 3.— SDSS and Keck spectra of the inactive M7 dwarf SDSS094738.45+371016.5 (a and b respectively) and the active M7 dwarf SDSS162718.20+353835.7 (c and d). Dashed lines in the SDSS spectra (a and c) indicate the expected position of the $\text{H}\alpha$ emission line. The inset panels in the SDSS spectra are zoomed in on the $\text{H}\alpha$ region (6500–6600 \AA). Despite their high quality, it is clear that no $\text{H}\alpha$ emission is detected in either of the inactive spectra.

dwarfs (Lépine et al. 2003; Burgasser & Kirkpatrick 2006; West et al. 2008). The combination of these indices ($\text{CaH2}+\text{CaH3}$ vs. TiO5) has been used to separate the dwarf population ($[\text{Fe}/\text{H}]\sim 0$) from the subdwarf population ($[\text{Fe}/\text{H}]\sim -1$). We include the index value for each molecular band in Table 1. All of the index values are consistent with disk dwarf metallicity (near Solar).

3.2.3. Dynamics

We assigned a Galactic population to each star using the 3-D space motions computed in West et al. (2008) and the criteria of Leggett (1992), where young disk stars (YD) have $-20 < U < 50$, $-30 < V < 0$, and $-25 < W < 10$. Stars outside this ellipse or with $|W| > 50$ are old disk (OD) and stars near the edge but with $|W| < 50$ are

classified as young-old disk stars (YOD). All of the dynamic classifications are included in Table 1. While our sample includes all 3 of the components, it is dominated by the old disk and young old disk populations; 12 of 14 stars are OD or YOD.

4. OBSERVATIONAL RESULTS

Six of the fourteen M6-M7 dwarfs in our sample have detectable rotation. Three of the rotating stars have measurable activity but the other 3 show no signs of activity in any of the emission lines in either the SDSS or Keck spectra. The cross-correlation shown in Figure 2 (SDSS094738.45+371016.5) is an example of one of the inactive M7 dwarfs that appears to be rotating despite not being magnetically active.

Figure 4 shows $L_{H\alpha}/L_{bol}$ (activity) as a function of $v \sin i$ for the M6-M7.5 dwarfs from this paper (filled symbols) and previous studies (Delfosse et al. 1998; Mohanty & Basri 2003; Reiners 2007, open diamonds). $L_{H\alpha}/L_{bol}$ values were calculated from EW measurements using the χ conversions of Walkowicz et al. (2004). Our sample includes M6-M7 dwarfs with both measured rotation as well as activity from the SDSS and Keck spectra (filled circles), measured rotation and activity from the Keck spectra (CaII K detected in SDSS; filled diamonds), activity from the Keck spectra but no rotation (filled triangles), activity from the SDSS spectra but no rotation (filled squares), no rotation or activity (horizontally aligned dots) and measured rotation but no activity (filled stars). Upper limits in both velocity and activity denote the levels to which our sample (and previous studies) could probe. All previous M6-M7.5 dwarfs were found to be active, while 9 of the 14 stars in our sample show no activity in either the SDSS or Keck spectra. The lack of activity is not surprising since that was our main selection criterion, however it highlights the fact that we are probing a sample with very different properties than previously studied.

The two most active stars in our sample are also the fastest rotators, and 6 of the inactive stars have no detectable rotation. Two of the active stars show no sign of rotation, which may be due to inclination effects (although the incidence in that case would be higher than statistically expected, if such small numbers can be said to have any significance).⁵ A similar excess of active non-rotators was found by Browning et al. (2008) at spectral types M3-M5. All 6 of the stars with detectable rotation have estimated Rossby numbers that are beyond (smaller than, by an order of magnitude) the activity “saturation” threshold of $R_0=0.1$ discussed in Reiners et al. (2008, the stars would need to have $V_{rot} < 0.7 \text{ km s}^{-1}$ to have $R_0 > 0.1$). However, none of these rotators show activity at the “saturated” level of $L_{H\alpha}/L_{bol} \sim 10^{-4}$. Most intriguing are the three M7 dwarfs that show no activity but are clearly detected rotators. We discuss this in more detail in §5.

Neither the metallicity nor dynamic population analyses reveal any significant trends with either rotation velocity or activity. This is not surprising, since both mea-

surements are only relevant in a statistical sense. However, all but one of the stars with a detected rotation comes from the YD or YOD population, and the one rotating OD shows no signs of activity (as do one of each from the other two populations).

5. DISCUSSION

We conducted high resolution spectral observations of 14 M6-M7 dwarfs and found $v \sin i$ rotation velocities for 6 for the stars. Three of the stars showed both activity and rotation, 6 of the stars showed neither rotation nor activity, 2 of the stars showed activity but no rotation and 3 stars showed rotation but no activity. These results are in contrast with previous studies that found a strong connection between rotation and activity in all (active) M6-M7 dwarfs (Delfosse et al. 1998; Mohanty & Basri 2003; Reiners 2007). As can be seen in Figure 4, those studies produced one out of 20 stars which was active but not rotationally broadened (very reasonably explained by the inclination effect; there is a 94% chance of selecting one out of 20 with the inclination needed to take it from 4 km s^{-1} to 2 km s^{-1}), and one which showed rotation and low (but not zero) activity. Our sample is the first rotation study to include by design M6-M7 dwarfs that are inactive.

Whereas previous studies sampled a range of dynamic populations and therefore stellar ages (Delfosse et al. 1998; Mohanty & Basri 2003), our sample was selected from a more distant, mostly inactive and potentially older population (M7 dwarfs have activity lifetimes of $\sim 8 \text{ Gyr}$; West et al. 2008). Although our sample is not representative of the entire M6-M7 population, it does examine a different part of parameter space than previously sampled and observes something not previously seen: rotation in inactive M7 dwarfs. Currently, there is no clear explanation for the rotation-activity patterns seen in our sample. However, we present a number of possible explanations that may account for this unusual dataset.

One possible explanation is that rotation and activity are not strongly linked in the fully convective envelopes of M6-M7 dwarfs. Previous studies only examined active M6-M7 dwarfs, many of which have activity levels with no notable correlation with rotation beyond a general tendency for rotators to lie in a broadly spread “saturated” activity regime. In fact, several active dwarfs have no detectable rotation (see Figure 4). Besides saturation, another explanation for the lack of a strong relationship between activity and rotation is inclination; the rotation axes of the stars may be inclined and therefore have reduced line-of-sight components to their rotation velocities. On the other hand, the 3 inactive stars with detected rotations certainly cannot be resolved by simply imposing inclination effects, which can only serve to make their true rotations even higher.

Another possibility is that there is a rotationally-induced threshold for activity at $V_{rot} > 6 \text{ km s}^{-1}$ (Hawley et al. 1996). This would explain the inactive rotators (they are below the threshold) and require that active stars with $v \sin i$ rotation velocities less than the threshold have inclined rotation axes. Combining all of the previous rotation studies for M6-M7 (Figure 4), we see that 7 of the 26 active dwarfs have $v \sin i \leq 6 \text{ km s}^{-1}$; the rest of the stars are rotating several km s^{-1} above the de-

⁵ Using the statistical formalism outlined in Browning et al. (2008), the probability of selecting 2 out of 5 active stars with the inclination required to alter their observed $v \sin i$ velocities from the mean detected velocity of 6 km s^{-1} to 3.5 km s^{-1} (non-detection) is 24%.

TABLE 2
MEASURED ATTRIBUTES II

Name	Spec. Type	$v \sin i$ (km s^{-1})	$L_{H\alpha}/L_{bol}^a$ ($\times 10^{-6}$)	$L_{H\alpha}/L_{bol}^b$ ($\times 10^{-6}$)	$L_{H\beta}/L_{bol}^a$ ($\times 10^{-6}$)	$L_{H\gamma}/L_{bol}^a$ ($\times 10^{-6}$)	$L_{H\delta}/L_{bol}^a$ ($\times 10^{-6}$)	L_{CaIIK}/L_{bol}^a ($\times 10^{-6}$)	Dyn. ^c Pop.
SDSS011012.22-085627.5	M7	<3.5	<1.0	<1.0	<0.5	<0.3	<0.9	<0.2	YOD
SDSS021749.99-084409.4	M6	4.0 ± 0.5	<2.0	<2.0	<1.4	<2.4	<1.5	<0.8	YD
SDSS023908.41-072429.3	M7	<3.5	<0.5	1.6	<0.6	<1.4	YOD
SDSS072543.94+382511.4	M7	<3.5	<0.5	<0.5	<0.2	<0.1	<0.1	<0.2	OD
SDSS083231.52+474807.7	M6	4.0 ± 0.5	<2.0	69.0	<0.7	<0.6	<0.5	1.1	OD
SDSS094720.07-002009.5	M7	6.5 ± 0.5	18.0	21.0	3.4	3.4	0.52	2.4	YOD
SDSS094738.45+371016.5	M7	6.0 ± 0.5	<1.0	<0.5	<0.2	<0.2	<0.4	<0.2	OD
SDSS110153.86+341017.1	M7	<3.5	<1.0	<0.5	<0.2	<0.2	<0.2	<0.2	OD
SDSS112036.08+072012.7	M7	<3.5	<0.5	<0.5	<0.2	<0.1	<0.1	<0.1	OD
SDSS125855.13+052034.7	M7	<3.5	4.68	<0.5	1.4	1.4	0.90	1.2	OD
SDSS151727.72+335702.4	M7	4.5 ± 0.5	<1.0	<0.5	<0.2	<0.1	<0.2	<0.1	YOD
SDSS162718.20+353835.7	M7	8.0 ± 0.5	31.0	28.0	16.0	7.4	6.5	5.3	YOD
SDSS220334.10+130839.8	M7	<3.5	<0.5	<0.5	<0.5	<0.6	<0.5	<0.4	YD
SDSS225228.50-101910.9	M7	<3.5	<1.0	<1.0	<0.6	<2.0	YOD

NOTE. — The L_{line}/L_{bol} values were calculated using the χ conversion factors derived by Walkowicz et al. (2004) and West & Hawley (2008).

^aEquivalent width or 3σ upper limit measured from the SDSS spectrum

^bEquivalent width or 3σ upper limit measured from the Keck spectrum

^cDynamical Populations based on the criteria in Leggett (1992)

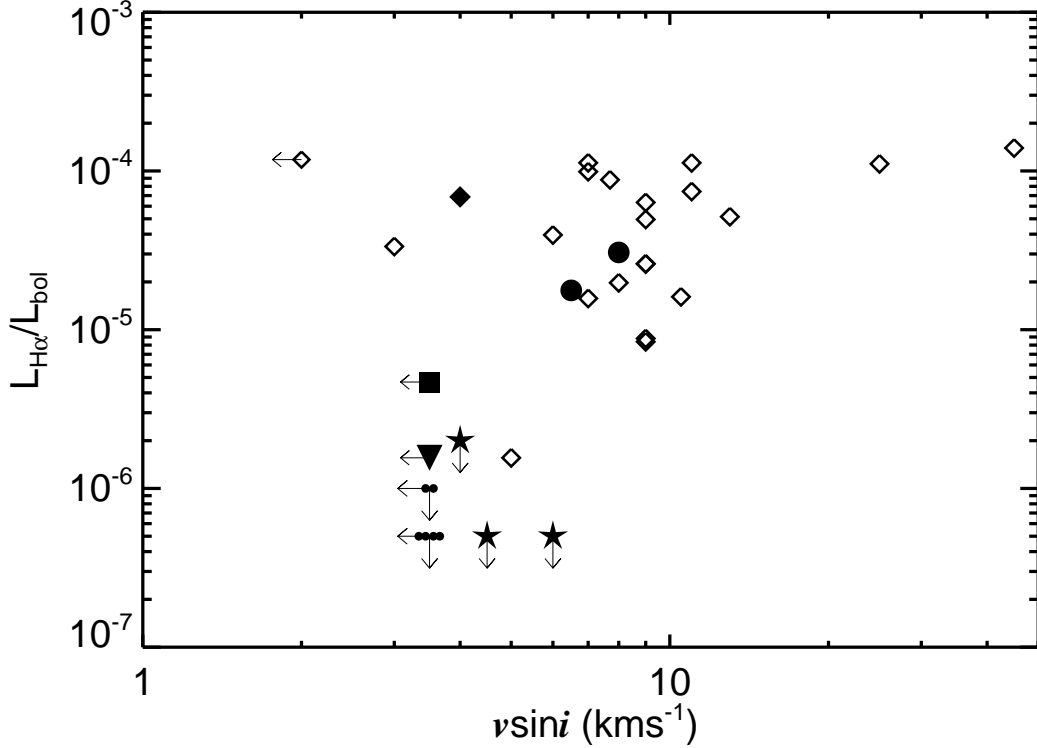


FIG. 4.— $L_{H\alpha}/L_{bol}$ (activity) as a function of $v \sin i$ (rotation) for the M6-M7.5 dwarfs from this paper (filled symbols) and previous studies (Delfosse et al. 1998; Mohanty & Basri 2003; Reiners 2007, open diamonds). $L_{H\alpha}/L_{bol}$ values were calculated from equivalent width measurements using the χ conversions of Walkowicz et al. (2004). Our sample includes M6-M7 dwarfs with both measured rotation as well as activity from the SDSS and Keck spectra (filled circles), measured rotation and activity from the Keck spectra (CaII K detected in SDSS; filled diamonds), activity from the Keck spectra but no rotation (filled triangles), activity from the SDSS spectra but no rotation (filled squares), no rotation or activity (horizontally aligned dots) and measured rotation but no activity (filled stars). Upper limits in both velocity and activity denote the levels to which our sample (and previous studies) could probe. All previous M6-M7.5 dwarfs were found to be active, while 9 of the 14 stars in our sample show no activity in either the SDSS or Keck spectra. The dearth of inactive late-type M dwarfs in previous studies is due to a selection effect that biases nearby samples to younger, more active stars (West et al. 2006, 2008). 3 of our stars show strong evidence for rotation despite having no activity. Their $v \sin i$ velocities are well above the 0.7 km s^{-1} required to have $R_0 > 0.1$ and be beyond the “saturated” regime (Reiners et al. 2008).

tection thresholds. To quantify this possibility, we follow the statistical analysis of Browning et al. (2008), where we compute the probability (from the binomial distribution) of observing n objects with inclination $i < i_{crit}$. We find that the probability of randomly drawing a sample of 7 stars with the inclinations necessary to take the slow but active stars from a $V_{rot}=6.5 \text{ km s}^{-1}$ to the observed $v \sin i$ is 85.7%. If we instead calculate the more conservative probability of drawing inclinations that take the 7 stars from 8 km s^{-1} (the median $v \sin i$) to their respective $v \sin i$ values, we obtain 55.9%. In this scenario, the inactive stars, which are presumably older, have spun down enough to fall below the rotation-activity threshold.

In earlier M dwarfs, the mere detection of rotation implies that the star is in the “saturation” regime; an effect that should have become even more pronounced for these even smaller objects (assuming the convective overturn time is similar). All of our detected rotators have estimated Rossby numbers that are beyond the “saturation” threshold for early-type M dwarfs (Reiners et al. 2008). One possibility is that in these fully convective late-type M dwarfs, the Rossby number “saturation” threshold might be substantially smaller. However, this model would imply that stars go from fully active to completely inactive over a small range of Rossby numbers - something that contradicts what is seen in early-type M dwarfs, where the activity falls smoothly with increasing Rossby number (Kiraga & Stepien 2007; Reiners et al. 2008). It is clear that the velocity thresholds proposed here would have to be lowered (as a function of spectral type) to be compatible with the results of Reiners et al. (2008); too many of their stars are active below $v \sin i = 6 \text{ km s}^{-1}$ (including several in the M5-6 spectral range).

Of course one additional possibility is that M6-M7 dwarfs might have activity cycles and that we are observing the inactive stars at a minimum in their cycles. Although this might be observed for a small number of stars, it is unlikely that an activity minimum can explain the majority of inactive M dwarfs seen in the Milky Way. West et al. (2008) showed that the activity fractions of M dwarfs are strongly correlated with the height above the Galactic plane (and therefore age), a trend that cannot be explained by an activity cycle.

The dearth of a large sample of nearby, inactive late-type dwarfs precludes large-scale follow-up that would further test the age-rotation-activity relation of fully convective low-mass dwarfs. However, future efforts to extend our analysis to both inactive M5 and M8 dwarfs will help elucidate the problem. The multi-epoch photometric observations produced by all sky time-resolved surveys (e.g. Pan-STARRS and LSST) will produce rotation periods for a large number of late-type M dwarfs

that will eliminate the inclination effects. Of course, inactive M dwarfs present a problem to this method in that they may not exhibit photometric variability (if they don’t produce starspots). The combination of these and other future observations will help advance the understanding of what role rotation plays in the production of magnetic fields in fully convective objects, and provide crucial constraints for theoretical models of fully convective dynamos. They will also be a key component to understanding the feedback between magnetic fields and stellar angular momentum evolution through stellar activity.

6. ACKNOWLEDGMENTS

The authors would like to thank Matt Browning, Ansgar Reiners, Suzanne Hawley, Lucianne Walkowicz, Kevin Covey, Adam Burgasser and John Bochanski for useful discussions while conducting this study.

G.B. acknowledges support from the NSF through grant AST-0606748. Some of the data presented herein were obtained at the W.M. Keck Observatory, which is operated as a scientific partnership among the California Institute of Technology, the University of California and the National Aeronautics and Space Administration. The Observatory was made possible by the generous financial support of the W.M. Keck Foundation.

Funding for the Sloan Digital Sky Survey (SDSS) and SDSS-II has been provided by the Alfred P. Sloan Foundation, the Participating Institutions, the National Science Foundation, the U.S. Department of Energy, the National Aeronautics and Space Administration, the Japanese Monbukagakusho, and the Max Planck Society, and the Higher Education Funding Council for England. The SDSS Web site is <http://www.sdss.org/>.

The SDSS is managed by the Astrophysical Research Consortium (ARC) for the Participating Institutions. The Participating Institutions are the American Museum of Natural History, Astrophysical Institute Potsdam, University of Basel, University of Cambridge, Case Western Reserve University, The University of Chicago, Drexel University, Fermilab, the Institute for Advanced Study, the Japan Participation Group, The Johns Hopkins University, the Joint Institute for Nuclear Astrophysics, the Kavli Institute for Particle Astrophysics and Cosmology, the Korean Scientist Group, the Chinese Academy of Sciences (LAMOST), Los Alamos National Laboratory, the Max-Planck-Institute for Astronomy (MPIA), the Max-Planck-Institute for Astrophysics (MPA), New Mexico State University, Ohio State University, University of Pittsburgh, University of Portsmouth, Princeton University, the United States Naval Observatory, and the University of Washington.

REFERENCES

- Adelman-McCarthy, J. K., et al. 2008, ApJS, 175, 297
- Barry, D. C. 1988, ApJ, 334, 436
- Browning, M. K. 2008, ApJ, 676, 1262
- Browning, M. K., Basri, G., Marcy, G. W., West, A. A., & Zhang, J. 2008, AJ, submitted
- Burgasser, A. J., & Kirkpatrick, J. D. 2006, ApJ, 645, 1485
- Chabrier, G., & Baraffe, I. 1997, A&A, 327, 1039
- Covey, K. R., et al. 2007, AJ, 134, 2398
- Delfosse, X., Forveille, T., Perrier, C., & Mayor, M. 1998, A&A, 331, 581
- Dobler, W., Stix, M., & Brandenburg, A. 2006, ApJ, 638, 336
- Gizis, J. E., Monet, D. G., Reid, I. N., Kirkpatrick, J. D., Liebert, J., & Williams, R. J. 2000, AJ, 120, 1085
- Gray, D. F. 1992, Science, 257, 1978
- Hawley, S. L., Gizis, J. E., & Reid, I. N. 1996, AJ, 112, 2799
- Kiraga, M., & Stepien, K. 2007, Acta Astronomica, 57, 149
- Leggett, S. K. 1992, ApJS, 82, 351
- Lépine, S., Shara, M. M., & Rich, R. M. 2003, ApJ, 585, L69
- Mamajek, E. E., & Hillenbrand, L. A. 2008, ApJ, in press
- Mohanty, S., & Basri, G. 2003, ApJ, 583, 451
- Ossendrijver, M. 2003, A&A Rev., 11, 287
- Parker, E. N. 1993, ApJ, 408, 707

- Pizzolato, N., Maggio, A., Micela, G., Sciortino, S., & Ventura, P. 2003, *A&A*, 397, 147
- Reid, I. N., Hawley, S. L., & Gizis, J. E. 1995, *AJ*, 110, 1838
- Reid, N., & Hawley, S. L., eds. 2005, *New light on dark stars : red dwarfs, low mass stars, brown dwarfs*, ed. N. Reid & S. L. Hawley
- Reiners, A. 2007, *A&A*, 467, 259
- Reiners, A., & Basri, G. 2007, *ApJ*, 656, 1121
- Reiners, A., Basri, G., & Browning, M. K. 2008, *ApJ*, in press
- Skumanich, A. 1972, *ApJ*, 171, 565
- Soderblom, D. R., Duncan, D. K., & Johnson, D. R. H. 1991, *ApJ*, 375, 722
- Thompson, M. J., Christensen-Dalsgaard, J., Miesch, M. S., & Toomre, J. 2003, *ARA&A*, 41, 599
- Walkowicz, L. M., Hawley, S. L., & West, A. A. 2004, *PASP*, 116, 1105
- West, A. A., Bochanski, J. J., Hawley, S. L., Cruz, K. L., Covey, K. R., Silvestri, N. M., Reid, I. N., & Liebert, J. 2006, *AJ*, 132, 2507
- West, A. A., & Hawley, S. L. 2008, *PASP*, 120, 1161
- West, A. A., Hawley, S. L., Bochanski, J. J., Covey, K. R., Reid, I. N., Dhital, S., Hilton, E. J., & Masuda, M. 2008, *AJ*, 135, 785
- West, A. A., et al. 2004, *AJ*, 128, 426